PROCEEDINGS OF SCIENCE

Towards Understanding the Origin of Cosmic-Ray Positrons

Zhili Weng[*†]
Massachusetts Institute of Technology, Cambridge, USA
E-mail: zhili.weng@cern.ch

Precision measurements of cosmic ray positrons by the Alpha Magnetic Spectrometer on the International Space Station are presented up to 1 TeV based on 1.9 million positrons. The positron flux exhibits a significant excess starting from 25.2 ± 1.8 GeV followed by a sharp drop-off above 284^{+91}_{-64} GeV. In the entire energy range the positron flux is well described by the sum of a diffuse term associated with low energy secondary positrons produced in the collision of cosmic rays, and a new source term of high energy positrons with a finite energy cutoff. The finite cutoff energy of the source term, E_s, is established with a significance of more than 4σ, and it's value is determined to be $E_s = 810^{+310}_{-180}$ GeV. These experimental data on cosmic ray positrons show that, at high energies, they predominantly originate either from dark matter collisions or from new astrophysical sources.

36th International Cosmic Ray Conference -ICRC2019-
July 24th - August 1st, 2019
Madison, WI, U.S.A.

[*] Speaker.
[†] on behalf of the AMS Collaboration

© Copyright owned by the author(s) under the terms of the Creative Commons Attribution-NonCommercial-NoDerivatives 4.0 International License (CC BY-NC-ND 4.0).

PoS(ICRC2019)091

Studies of light cosmic ray antimatter species, such as positrons, antiprotons, and antideuterons, are crucial for the understanding of new physics phenomena in the universe, since the flux of these particles from secondary production of primary cosmic ray collisions with intterstellar matter is small [1]. There has been widespread interest and various explanations [2, 3, 4] of the observed excess of high energy positrons [5]. Most of these explanations differ in their predictions for the behavior of cosmic ray positrons at high energies.

In this proceeding we present precision measurements of the positron flux and electron flux up to 1 TeV measured with the Alpha Magnetic Spectrometer (AMS) on the International Space Station (ISS) [6]. The measurements are based on 1.9 million positron events collected by AMS from May, 2011 to Nov, 2017. The AMS observation of distinctive properties of positron fluxes are crucial for understanding the origin of high energy positrons in the cosmos and for providing insights into new physics phenomena.

1. AMS-02 Detector

The full description of the AMS detector is presented in Ref. [6] and references therein. The key detector elements used for the positron analysis are the transition radiation detector TRD, the time of flight counters TOF, the silicon tracker, the permanent magnet, and the electromagnetic calorimeter ECAL.

The tracker has nine layers, the first layer, $L1$, at the top of the detector, the second layer, $L2$, above the magnet, six layers, $L3$ to $L8$, within the bore of the magnet, and the last layer, $L9$, above the ECAL. Together with the magnet, the tracker accurately determines the particle trajectory and measures rigidity R (momentum/charge). The maximum detectable rigidity, MDR, is 2 TV for $|Z| = 1$ particles over the 3 meters lever arm from $L1$ to $L9$. The tracker also measure the particle charge $|Z|$ with charge resolution of $\Delta Z \simeq 0.05$. The TOF measures $|Z|$ with a resolution $\Delta Z \simeq 0.05$ and velocity β with a resolution of $\Delta\beta/\beta^2 = 4\%$. The TRD separates electron (e^-) and positron (e^+) from protons (p) using 20 layers proportional tubes. The TRD estimator Λ_{TRD} is constructed from the ratio of the log–likelihood probability of the $e^\pm$ hypothesis to that of the p hypothesis in each layer. The ECAL has 17 radiation length. It's 3-dimensional imaging capability allows for an accurate measurement of the positron energy and of the shower shape. To identify positron from proton, an ECAL estimator Λ_{ECAL} [7] is used to differentiate $e^\pm$ from p by exploiting their different shower shapes.

To distinguish positrons from charge confusion electrons, that is, electrons which are reconstructed in the tracker with positive rigidity, a charge confusion estimator Λ^e_{CC} is defined [6, 8]. This technique allows for efficient separation between positron signal and electron charge confusion background.

The entire detector has been extensively calibrated in a test beam at CERN with measurements in 18 different energies and particles at 2000 positions. This provides detail understanding of the performance of the full AMS detector. The calibration is also extended to higher energies with the cosmic ray proton data. The detector performance on orbit is continuously monitored and it is steady over time.

PoS(ICRC2019)091

A Monte Carlo program using the GEANT4 10.1 package [9] is developed based on the results of extensive calibrations both on the ground and in space. This program simulate physics processes and signals in the detector and provides an excellent description of the data.

2. Positron Measurement

The full analysis procedure for positron flux measurement is described in detailed in Ref. [6]. After event selections, the positive rigidity event sample is comprised of positron signal, proton background, and charge confusion electron background. The combination of information from the TRD, tracker, and ECAL enables the efficient separation of the positron signal events from background events using a template fitting technique. First, to remove the bulk of the proton background, an energy dependent cut on ECAL estimator Λ_{ECAL} is applied. The number of positrons in each bin are then determined by fitting signal and background templates to data in the two dimensional variable space of $(\Lambda_{\mathrm{TRD}} - \Lambda^{e}_{\mathrm{CC}})$ by varying their respective normalization. This method allows for determination of number of positron signal, proton background and electron charge confusion background events simultaneously from the data sample. In total, 1.9 million positrons in the energy range from 0.5 GeV to 1 TeV.

The isotropic positron flux for the energy bin E_i of width ΔE_i at the top of AMS is calculated by:

$$\Phi_{e^+,i} = \frac{N_i}{A_i(1+\delta_i)T_i\Delta E_i}, \tag{1}$$

where N_i is the number of e^+ in the energy bin i corrected for the small bin-to-bin migration using the unfolding procedure described in Ref. [10]. A_i is the effective acceptance calculated from MC simulation. T_i is the data collection time. δ_i is minute corrections estimated by comparing the efficiencies in data and MC simulation of every selection cut using information from the detectors unrelated to that cut.

Detailed study of the systematic errors is key part of the analysis. Systematic uncertainties for the positron flux include uncertainties from: template definition, charge confusion determination, efficiency correction, bin-to-bin migration and energy scale. These are discussed in detailed in Ref. [6].

One of the most important systematic error come from electron charge confusion. The level of charge confusion is determined directly from data using the information from the charge confusion estimator. The amount of charge confusion is well reproduced by the Monte Carlo simulation. The electron charge confusion fraction (defined as the fraction of electron events being reconstructed as positive rigidity after final selection) at 1TV is 8%. The corresponding systematic error accounts for the small differences between data and the Monte Carlo simulation. This error is negligible below 200 GeV, 3% at $[370-500]$ GeV, and 18% at $[700-1000]$ GeV.

The AMS ECAL provide precision energy measurement of positrons [7]. The energy scale error is 4% at 0.5 GeV, 2% from 2 to 300 GeV, and 2.5% at 1 TeV. This is treated as an uncertainty of the bin boundaries.

Most importantly, starting from 30 GeV statistical error becomes dominating the total error. Therefore by continuing taking data, AMS will be able to improve the accuracy of the measurement and reach into uncharted high energy range.

PoS(ICRC2019)091

3. Distinctive Properties of Positron Flux

Figure 1 shows the measured AMS positron spectrum (defined here as the flux scaled by E^3). The error bars correspond to the quadratic sum of statistical and systematic errors [6]. As seen, the precision AMS measurement show distinct energy dependence of the positron spectrum: the average positron spectrum is flattening from 7.10 to 27.25 GeV (green vertical band). from 27.25 to 290 GeV the positron spectrum exhibits significant rise (orange vertical band); at ∼290 GeV the positron spectrum reached a maximum followed by a sharp drop-off (blue vertical band).

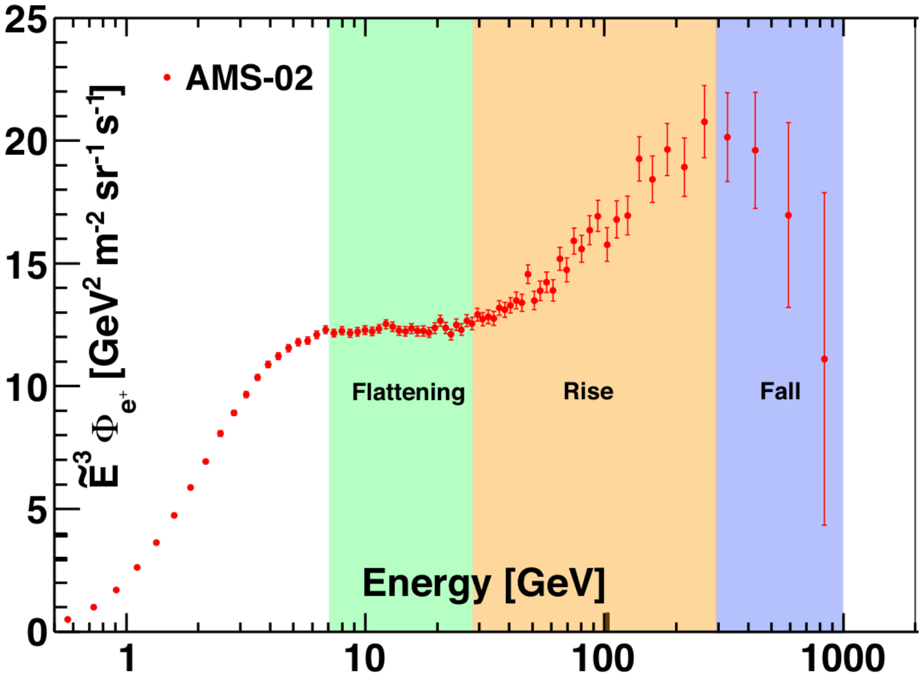

Figure 1: For display purposes, the positron flux, Φ_{e^+} is presented scaled by $\tilde{E}^3$. The resulting positron spectrum, $\tilde{E}^3\,\Phi_{e^+}$, (red data points) is shown as a function of energy $\tilde{E}$. To guide the eye, the vertical color bands indicate the energy ranges corresponding to changing behavior of the spectrum: flattening, rising(hardening), and falling(softening) spectrum.

This complex energy dependence of the positron spectrum can be further studied in a model independent way by calculating the flux spectral index γ:

$$\gamma = d[\log(\Phi_{e^+})]/d[\log(E)], \tag{2}$$

The AMS positron flux spectral index over non-overlapping energy intervals are presented in Fig. 2. The positron flux spectral index is not a constant and it exhibits complex behavior as function of energy. It decreases (soften) rapidly from ∼3 GeV to ∼7 GeV. In the energy range $[7.10-27.25]$ GeV it reaches a local minimum with an average $\gamma = -2.99 \pm 0.01$. It then rises(harden) to an local maximum of $\gamma = -2.72 \pm 0.04$ in the energy range $[55.58-148.81]$ GeV. Above 148.81 GeV the spectral index experiences significant decrease reaching $\gamma = -3.35 \pm 0.32$ in the highest energy interval $[290-1000]$ GeV.

PoS(ICRC2019)091

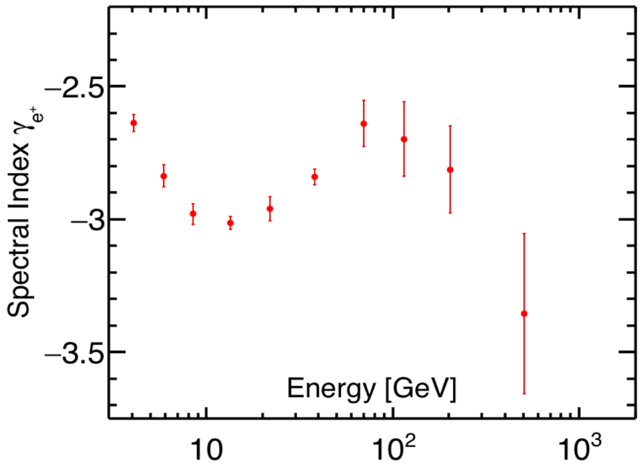

Figure 2: The spectral index of the AMS positron flux in non-overlapping energy intervals (red data points). The spectral index has complex energy dependence with a significant decrease towards higher energies.

To determine the transition energy E_0 where the spectral index starts rising, we use a double power law function:

$$\Phi_{e^+}(E) = \begin{cases} C(E/55.58\,\mathrm{GeV})^{\gamma}, & E \leq E_0; \\ C(E/55.58\,\mathrm{GeV})^{\gamma}(E/E_0)^{\Delta\gamma}, & E > E_0. \end{cases} \tag{3}$$

A fit to data in the energy range $[7.10 - 55.58]$ GeV are presented in Fig. 3a. The fit yields $E_0 = 25.2 \pm 1.8$ GeV for the energy where the spectral index increases, with $\chi^2/\mathrm{d.o.f.} = 23/31$. The significance of this increase is established at more than 6σ. The energy E_0 corresponds to the start of a significant excess of the positron flux compared to the lower energy trends.

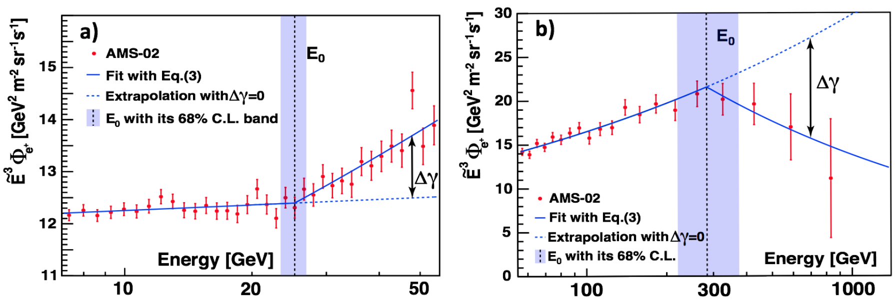

Figure 3: A double power law fit of Eq. (3) to the flux in the energy ranges $[7.10 - 55.58]$ GeV and $[55.58 - 1000]$ GeV, respectively. The red data points are the measured positron flux scaled by $\tilde{E}^3$. The fitted functions are represented by the blue lines. The vertical dashed lines and the bands correspond to E_0 and its error. The dashed blue lines are the extrapolations of the power law below E_0 into the higher energy regions. $\Delta\gamma$ is the magnitude of the spectral index change.

Similarly, to determine the transition energy where the spectral index starts decreasing, a fit to the data in the energy range $[55.58 - 1000]$ GeV are presented in Fig. 3b. The fit yields $E_0 =$

PoS(ICRC2019)091

284^{+91}_{-64} GeV for the energy of the spectral index decrease and $\chi^2/\text{d.o.f.} = 13/16$. The significance of the spectral index decrease at 284^{+91}_{-64} GeV is established at more than 3σ.

At energy starting from ~ 10 GeV, the AMS positron flux by far exceeds the contribution from secondary origin produced from collision of cosmic rays with the interstellar gas [11], primary source of positrons is needed to describe the observed positron excess. Models to explain the primary source of cosmic ray positron includes annihilation of Dark Matter particles [2] and other astrophysical objects like super nova remnants or pulsars [3]. The accuracy of the AMS data allows for a detailed study of the properties of the new source of positrons up to 1 TeV. As an example we use a minimal model [5, 6] to analyze the origin of different sources of positron. In this model, the positron flux Φ_{e^+} is parameterized as the sum of a diffuse term and a source term:

$$\Phi_{e^+}(E) = \frac{E^2}{\hat{E}^2}[C_d\,(\hat{E}/E_1)^{\gamma_d} + C_s\,(\hat{E}/E_2)^{\gamma_s}\exp(-\hat{E}/E_s)]\,. \tag{4}$$

The diffuse term is a power law function, which describes the secondary positrons produced in the collisions of primary cosmic rays with the interstellar gas. It is characterized by a normalization factor C_d and a spectral index γ_d. This contribution is expected to dominate at low energy. The source term is a power law function with an exponential cutoff, which describes the high energy part of the flux dominated by a source. It is characterized by a normalization factor C_s, a spectral index γ_s, and a cutoff energy E_s. The force-field approximation [12] is used to account for solar modulation effect such that the energy of particles in the interstellar space $\hat{E} = E + \varphi_{e^+}$, where φ_{e^+} is the effective solar potential. The constant E_1 and E_2 does not affect the shapes nor the magnitudes of the two contribution and are chosen to be 7.0 GeV and 60.0 GeV respectively to minimize correlation between parameters. The fit of Eq. (4) to the measured flux yields the inverse cutoff energy $1/E_s = 1.23 \pm 0.34\,\text{TeV}^{-1}$ corresponding to $E_s = 810^{+310}_{-180}$ GeV and $\chi^2/\text{d.o.f.} = 50/68$. Other fitted parameters are: C_s = (6.80 $\pm$ 0.15) $\times 10^{-5}[\text{m}^2\,\text{sr}\,\text{s}\,\text{GeV}]^{-1}$, γ_s = -2.58 $\pm$ 0.05, C_d = (6.51 $\pm$ 0.14) $\times 10^{-2}[\text{m}^2\,\text{sr}\,\text{s}\,\text{GeV}]^{-1}$, γ_d = -4.07 $\pm$ 0.06 , φ_{e^+} = 1.10 $\pm$ 0.03 GeV.

The result of the fit is presented in Fig. 4, together with the contribution from different components. As seen, the diffuse term (grey filled area) dominates at low energies and gradually vanishes with increasing energy. The source term (magenta filled area) dominates the positron spectrum at high energies. This analysis shows that the observed excess of the positron flux above 25.2 ± 1.8 GeV is due to the existence of the source term.

The drop-off of the flux above 284 GeV is very well described by the exponential cutoff of the source term. The existence of a finite energy cutoff is crucial in understanding the nature of the new high energy source of positrons. To study the significance of the $1/E_s$ measurement, we varied all six fit parameters to establish confidence levels from 1 to 5σ with a step of 0.01σ. Fig. 5 shows the projection of the 6-dimension envelope of 1σ (green line, 68.26% C.L.), 2σ (black line, 95.54% C.L.), 3σ (blue line, 99.74% C.L.), and 4σ (red line, 99.99% C.L.) onto the plane of parameters $1/E_s - C_s$. This study shows that the point where the parameter $1/E_s$ reaches 0 corresponds to the confidence level of 4.07σ. Therefore, a source term without a exponential energy cutoff is excluded at more than at more than 4σ.

PoS(ICRC2019)091

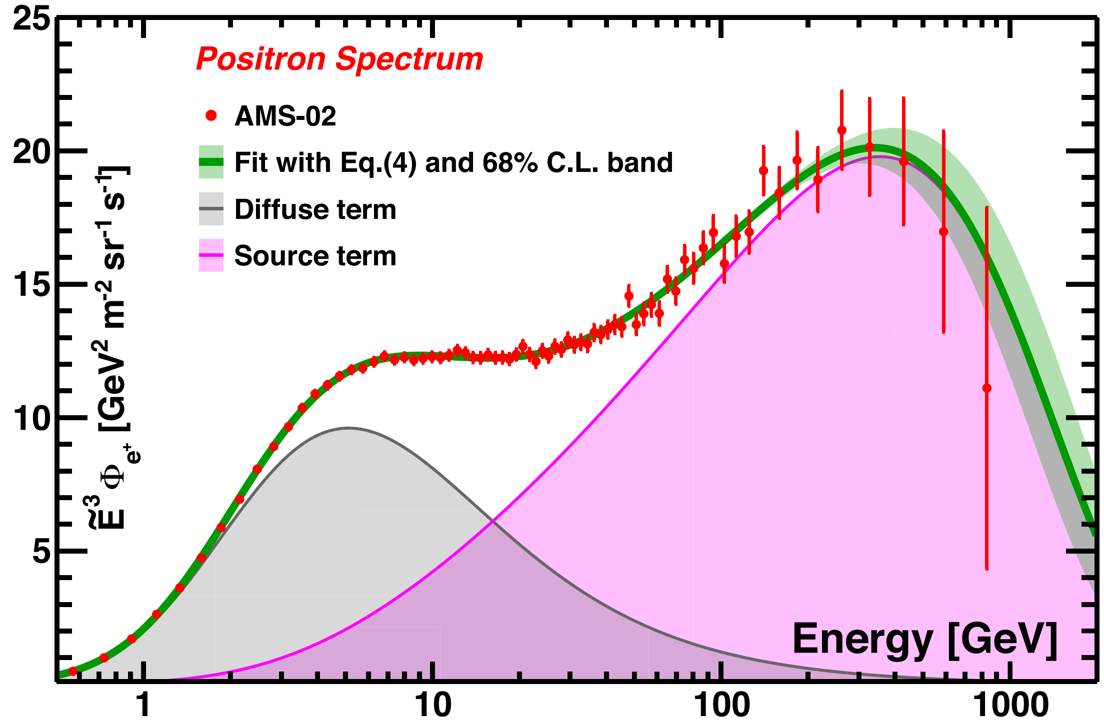

Figure 4: The fit of Eq. (4) (green line) to the positron flux in the energy range $[0.5-1000]$ GeV together with the 68% CL interval (green band). The red data points represent the measured average positron flux values over the measurement period scaled by $\tilde{E}^3$. The source term contribution is represented by the magenta area, and the diffuse term contribution by the grey area.

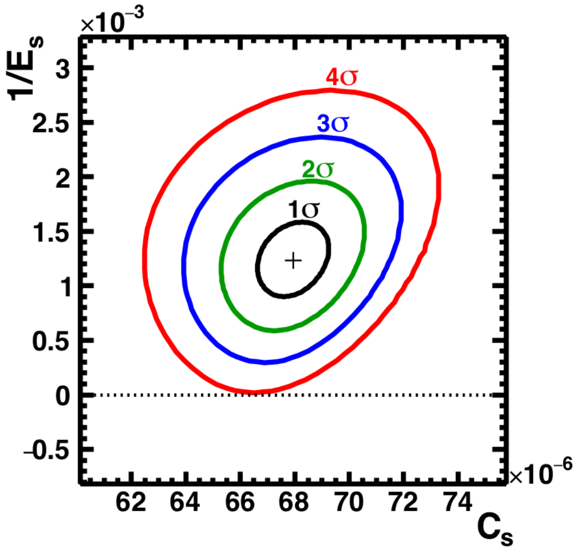

Figure 5: The projections of the regions of 1σ (green contour), 2σ (black contour), 3σ (blue contour), and 4σ (red contour) significance of the $1/E_s$ measurement onto the plane of parameters $1/E_s - C_s$ (see text).

PoS(ICRC2019)091

4. Conclusion

In conclusion, we have presented the precision measurements of cosmic ray positrons up to 1 TeV based on 1.9 million positrons. The positron flux exhibits complex energy dependence with a significant excess starting from 25.2 ± 1.8 GeV followed by a sharp drop-off above 284^{+91}_{-64} GeV. In the entire energy range the positron flux is well described by the sum of a diffuse term associated with low energy secondary positrons produced in the collision of cosmic rays, and a new source term of high energy positrons with a finite energy cutoff. The finite cutoff energy of the source term, E_s, is established with a significance of more than 4σ, and it's value is determined to be $E_s = 810^{+310}_{-180}$ GeV. These experimental data shows that, at high energies, cosmic ray positron predominantly originate either from dark matter collisions or from other astrophysical sources.

References

[1] F. Donato, N. Fornengo, and P. Salati, Phys. Rev. D **62** 043003 (2000); M. Cirelli, R. Franceschini, and A. Strumia, Nucl. Phys. B **800**, 204 (2008); P. Blasi. Phys. Rev. Lett. **103** 051104 (2009);

[2] M. S. Turner and F. Wilczek, Phys. Rev. D **42** 1001 (1990); J. Ellis, AIP Conf. Proc. **516**, 21 (2000); J. Kopp, Phys. Rev. D 88, 076013 (2013); L. Bergstrom *et al.*, Phys. Rev. Lett. 111, 171101 (2013);

[3] P. D. Serpico, Astropart. Phys. **39-40** 2 (2012); T. Linden and S. Profumo, Astrophys. J. **772**, 18 (2013); P. Mertsch and S. Sarkar, Phys. Rev. D **90**, 061301 (2014); I. Cholis and D. Hooper, Phys. Rev. D 88, 023013 (2013);

[4] R. Cowsik, B. Burch, and T. Madziwa-Nussinov, Astrophys. J. **786**, 124 (2014); K. Blum, B. Katz, and E. Waxman, Phys. Rev. Lett. **111**, 211101 (2013).

[5] M. Aguilar *et al.*, Phys. Rev. Lett. **110**, 141102 (2013); L. Accardo *et al.*, Phys. Rev. Lett. **113**, 121101 (2014). M. Aguilar *et al.*, Phys. Rev. Lett. **113**, 121102 (2014); M. Aguilar *et al.*, Phys. Rev. Lett. **113**, 221102 (2014).

[6] M. Aguilar *et al.*, Phys. Rev. Lett. **122**, 041102 (2019).

[7] A. Kounine, Z. Weng, W. Xu, and C. Zhang, Nucl. Instrum. Methods Phys. Res., Sect. A **869**, 110 (2017).

[8] M. Aguilar *et al.*, Phys. Rev. Lett. **117**, 091103 (2016);

[9] S. Agostinelli *et al.*, Nucl. Instrum. Methods Phys. Res., Sect. A **506**, 250 (2003); J. Allison *et al.*, IEEE Trans. Nucl. Sci. **53**, 270 (2006).

[10] M. Aguilar *et al.*, Phys. Rev. Lett. **114**, 171103 (2015);

[11] I. V. Moskalenko and A. W. Strong, Astrophys. J. **493**, 694 (1998); A. E. Vladimirov, S. W. Digela, G. Jóhannesson, P. F. Michelson, I. V. Moskalenko, P. L. Nolan, E. Orlando, T. A. Porter, and A. W. Strong, Comput. Phys. Commun. **182**, 1156 (2011).

[12] L. Gleeson and W. Axford, Astrophys. J. **154**, 1011 (1968).

PoS(ICRC2019)091